12-2015

Analysis of an electrospun nanofiber device applicable to limb salvage: mass loss, morphological changes, and quantification of antibiotic release

Caitlin Quinn

University of Tennessee at Chattanooga, myh692@mocs.utc.edu

Analysis of an Electrospun Nanofiber Device Applicable to Limb Salvage: Mass Loss, Morphological Changes, and Quantification of Antibiotic Release

Caitlin Quinn

Departmental Honors Thesis

The University of Tennessee at Chattanooga

Department of Chemistry

Project Director: Dr. Steven Symes

Examination Date: Thursday, March 26, 2015

Members of Examination Committee:

Dr. Robert Mebane

Dr. Andrew Ledoan

Dr. Jisook Kim

Examining Committee Signatures:

_____

Project Director

_____

Department Examiner

_____

Department Examiner

_____

Liaison, Departmental Honors Committee

_____

Chairperson, University Departmental Honors Committee

ABSTRACT

The creation of an electrospun nanofiber embedded with two antibiotics that will be used to prevent infection while also stimulating bone regeneration will be explored. The nanofiber will contain an aminoglycoside and a glycopeptide, and it is sought to deliver a sustained release of antibiotics for up to 12 weeks. To determine release rate, nanofiber samples are immersed in 10.0 mL of MiliQ water (MQ), incubated at 37°C, assayed at specific time intervals, and then analyzed using ultra performance liquid chromatography in tandem with mass spectrometry. A hydrophilic interaction liquid chromatography (HILIC) method utilizing ultra-performance liquid chromatography (UPLC) in tandem with mass spectrometry (MS) has been developed in order to quantify the release rate of each antibiotic from the nanofiber mesh as a function of time spent in MQ. The antibiotic release rate for six separate permutations of nanofibers was documented. In addition to monitoring drug release as a function of time, mass loss, pH changes, and morphology changes as a function of time have been monitored for an additional three antibiotic-free permutations of nanofiber devices. More specifically, the mass loss profiles for the three permutations of nanofiber devices were generated. To determine mass loss, nanofiber samples are immersed in 10.0 mL of a phosphate buffered saline (PBS), incubated at 37°C, assayed at specific time intervals, and then a final mass was directly compared to the starting mass. Changes in morphology were documented using a scanning electron microscope (SEM). SEM images were taken at weekly intervals and compared to original SEM images characterizing the nanofibers before immersion in PBS.

TABLE OF CONTENTS

LIST OF TABLES

LIST OF FIGURES

INTRODUCTION

Purpose

This study proposes to develop a liquid-chromatography mass-spectrometry (LC-MS) method to determine the time-resolved elution profile of two antibiotics incorporated in to a novel nanofiber based residue-free drug delivery device for management of orthopaedic infections. This device will be constructed by electrospinning bioresorbable synthetic polymer following incorporation of the antibiotics tobramycin and vancomycin. Optimization of pharmacokinetic properties by fine tuning process parameters (drug loading, nanofiber matrix porosity and fiber morphology) will result in controlled release of antibiotics from the device. The proposed device will provide local antibiotic therapy at a controlled rate for up to twelve weeks and will be resorbed following its function leaving behind healed natural bone as a function of time. It is believed that this drug delivery device will replace antibiotic beads used as standard of care for orthopedic infections.

The goal of the present project is to measure the rate at which antibiotics are released by the nanofiber devices. A specific release rate can be tailored for a desired therapeutic level via optimization of nanofiber characteristics (e.g. diameter, porosity, polymer used) and total mass of drug loaded in the device. Release rates of tobramycin and vancomycin will be monitored by incubation of the antibiotic-laden nanofibers under physiological conditions for defined time steps followed by quantitation of antibiotic levels released into the fluid. Additionally, mass loss of the nanofiber device as a function of time and morphological changes to the nanofiber device will be analyzed.

Existing Infection Control Methods

Following extensive orthopaedic surgery, the most typical problem facing the patient is bacterial infection. Originally introduced in 1970 by Buchholz and Engelbrecht, acrylic bone cement beads loaded with antibiotics are still commonly used today. The cement polymer used for the majority of acrylic bone beads is polymethylmethacrylate (PMMA). Antibiotic-containing PMMA beads are the most commonly used local antibiotic delivery system following orthopaedic surgery due to the documented ability of PMMA drug delivery devices to provide high concentrations of antibiotics to orthopaedic surgery sites that are usually poorly vascularized (Samuel et al. 2010). Additionally, antibiotic loaded PMMA cement beads provide high antibiotic concentrations at the infection site, but do not cause overall high levels of antibiotics in the patient's serum; lower levels of antibiotic in serum levels can result in a decrease in the probability of negative side effects (Barth et al. 2011).

While antibiotic PMMA beads can provide high concentrations of antibiotics at the site of infection, there is no definitive conclusion suggesting that antibiotic PMMA beads are actually effective at treating and/or preventing infection following orthopaedic surgery. In order to establish a direct connection between infection control and antibiotic PMMA beads, there ultimately needs to be more studies involving antibiotic-containing PMMA beads, preferably with larger sample sizes (Barth et al. 2011).

Documented negative aspects to the usage of antibiotic-containing PMMA beads include antibiotic resistance development and the bio-incompatibility of the PMMA cement beads themselves. The PMMA beads are not bioresorable, and therefore must be removed with a second surgery. A second surgery can allow for the onset of additional infection. If successful, the proposed device in this project will significantly transform the way infections are controlled;

the fact that the proposed nanofiber device will be bioresorbable eliminates the need for a second surgery required by PMMA beads. As any major surgery is accompanied by inherent risks and dangers, any opportunity to reduce the number of times a patient is operated on is significant. Secondly, antibiotic PMMA beads are known to aid in the development of antibiotic resistant bacteria. Bacteria have the ability to colonize on the surface of the PMMA beads, developing a biofilm which ultimately allows the PMMA beads to support the sustained presence of bacteria. This association between the PMMA beads and bacteria can lead to antibiotic resistant bacteria. For example, over 65% of the bacterial strains found on gentamicin PMMA beads removed after an orthopaedic surgery were gentamicin resistant (Barth et al. 2011).

Nanofibers Background

Nanofibers are composed of polymers ranging from biological polymers such as the nanofiber devices in this project to synthetic polymers such as nylon. The nanofibers analyzed in this project are electrospun nanofibers composed of poly(lactide-co-glycolide) (PLGA), a biological polymer of lactic and glycolic acids. Nanofibers are characterized by having fiber diameters in the several hundred nanometer range. For the sake of comparison, when compared to human hair, the diameter of a typical nanofiber is on the order of 200-900 nm, whereas the human hair has an average diameter of 100 µm. The SEM image below shows the drastic size difference between a human hair and a nanofiber sample; note that the human hair is laid atop the nanofiber sample.

Figure 1: Human Hair vs. Nanofiber SEM Image.

Nanofiber Composition

PLGA

The nanofiber device studied is composed 50:50 poly(lactic-co-glycolic acid) (PLGA), which is a Food and Drug Administration (FDA) approved, bioresorable copolymer of lactic and glycolic acids. 50:50 PLGA is a PLGA copolymer composed of equal amounts of lactic acid and glycolic acid monomers. PLGA has minimal toxicity since PLGA decomposes via hydrolysis to lactic and glycolic acids which are physiological metabolic pathway byproducts. During the hydrolysis of PLGA, water molecules interact directly with the ester bonds between chains as shown in Figure 2. The degradation rate of PLGA can be altered by altering the ratio of

lactic acid to glycolic acid; increasing the ratio of glycolide components to lactide components in the polymer increases the rate of degradation (Kim et al. 2004).

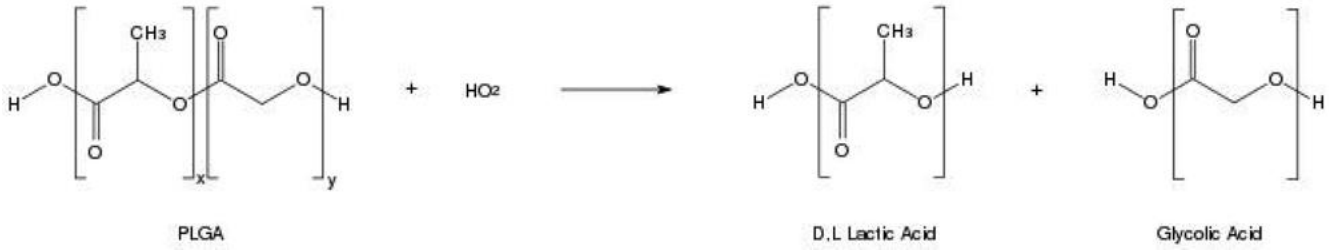

Figure 2: Hydrolysis of PLGA. The hydrolysis of PLGA produces lactic and glycolyic acids (Makadia et al. 2011).

Collagen

Collagens are key structural components of connective tissues such as tendons, ligaments, cartilage, and various membranes. Specifically, type I collagen will be incorporated into the nanofiber device proposed in this project. Overall, type I collagen is the most abundant of all types of collagen. 90% of all bone mass in the body is attributed to type I collagen. Type I collagen is an integral component of bone, tendon, and ligament, making it an overall important additive in the nanofiber device. More specifically however, type I collagen is an important component of the nanofiber device since type I collagen is responsible for many of the biomechanical characteristics of bone including overall bone strength (Friess 1998).

Hydroxyapatite

Hydroxyapatite (HA) is a naturally occurring mineral and a common component of both bone and teeth. The chemical formula for HA is $Ca_{10}(PO_4)_6(OH)_2$, and therefore HA is a

calcium apatite with a crystal cell composed of two $Ca_5(PO_4)_3(OH)$ units (Gao et al. 2006). HA has been shown to promote an increased rate of bone regeneration when incorporated into orthopaedic surgical devices; it is suggested that HA has a role in the induction mesenchymal cell differentiation towards osteoblasts which can ultimately lead to the formation of bone; therefore HA is advantageous to include in the nanofiber device proposed in this project (Yang et al. 1997).

Antibiotics

Vancomycin

Vancomycin is a glycopeptide antibiotic used to combat gram positive bacteria, being especially useful when combating methicillin resistant *staphylococci* (Zhang et al. 2007). Vancomycin works by inhibiting the cell wall formation in gram positive bacteria. The structure of vancomycin is given below in Figure 3 along with pK_a values (ChemAxon). The formula weight of vancomycin is 1449.3 amu and is characterized by the following functional groups: carboxylic acid, phenolic hydroxyl groups, amide groups, primary amine, and secondary amine. Overall, vancomycin is less hydrophilic than tobramycin, but is still characterized as both hydrophilic and polar.

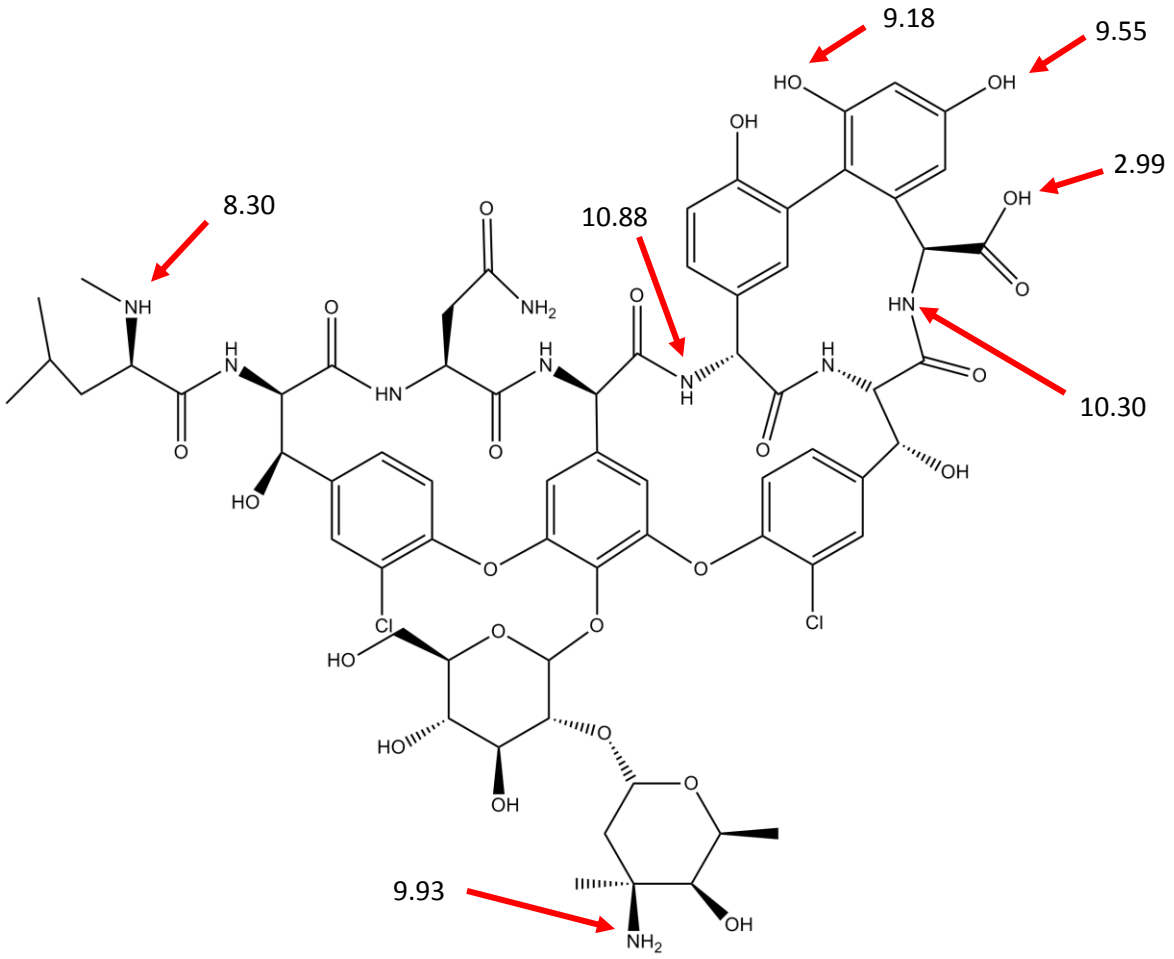

Figure 3: Vancomycin Structure and pK_a Values. At physiological pH (pH 7.4) it is important to note that vancomycin has a net charge of +1.

Tobramycin

Tobramycin is an aminoglycoside antibiotic. Tobramycin provides defense against gram negative bacteria, functioning by inhibiting bacterial DNA replication, specifically the translation of bacterial mRNA. Tobramycin is particularly effective against *Pseudomonas aeruginosa*. Aminoglycoside antibiotics are both nephrotoxic, harmful to the kidneys, and ototoxic, harmful to the ears (Barth et al. 2011). The formula weight for tobramycin is 467.5 amu. The structure of tobramycin along with the respective pK_a values for each amine group is shown below in Figure 4 (ChemAxon). From Figure 4, it is obvious that tobramycin is both polar and hydrophilic. Additionally, from the amine groups present, tobramycin is considered basic.

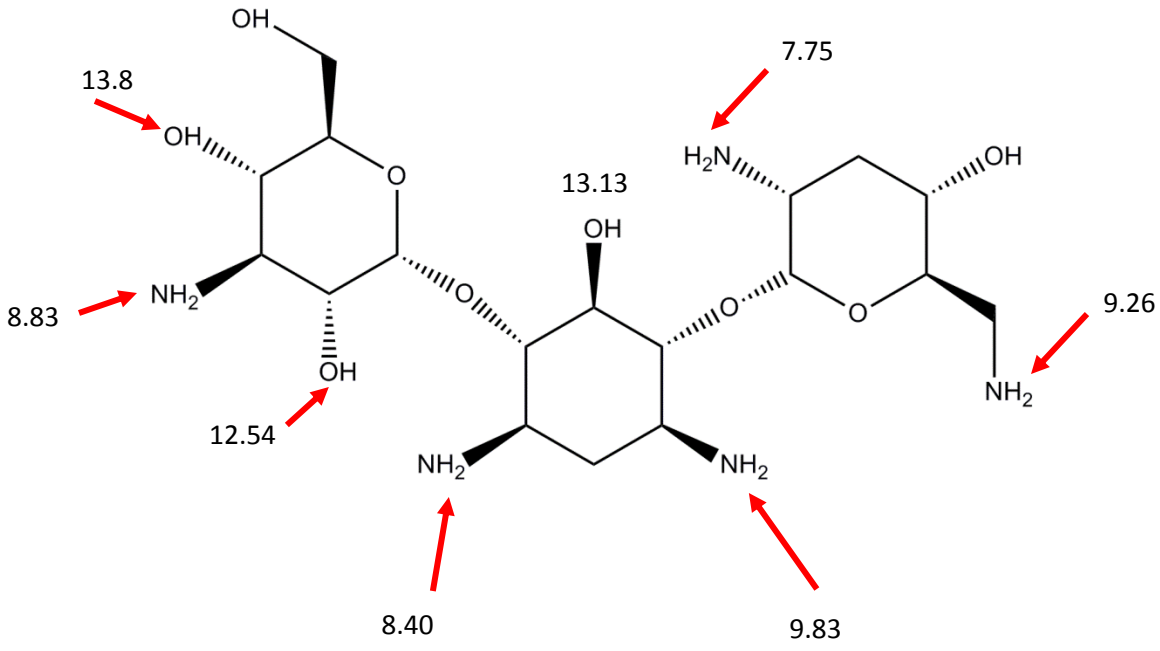

Figure 4: Tobramycin Structure with pK_a Values. At pH 7.4 tobramycin has a net charge of +5.

Phosphate-Buffered Saline (PBS)

In an attempt to mimic physiological conditions, a phosphate buffered saline solution was used. PBS is isotonic to human cells, containing ions such as K^+, Cl^-, Na^+, and $H_2PO_4^-$, and HPO_4^{2-}, and has a pH near the physiological pH of 7.4. Cellgro® PBS (cat. No. 21-030) with pH 7.0±0.1 and osmolality of 285±15 mOsm was purchased and used throughout the project. The composition of the PBS is given in Table 1.

Table 1: PBS Cat. No. 21-030 1X, Liquid

Inorganic Salts	*Concentration (g/L)*
$CaCl_2$ (anhydrous)	0.10
KCl	0.20
KH_3PO_4	0.20
$MgCl_2 \bullet 6H_2O$	0.10
NaCl	8.00
$Na_2HPO_4 \bullet 7H_2O$	2.1716

Analytical Techniques

To quantify the release rate of two antibiotics, tobramycin and vancomycin, from an electrospun nanofiber mesh this project utilized ultra performance liquid chromatography in tandem with mass spectrometry. Liquid chromatography was chosen specifically because the antibiotics will be eluted into a liquid matrix and in order to properly quantify the concentrations of each individual antibiotic, the two antibiotics will need to be separated from

both the matrix and one another. Ultra performance liquid chromatography (UPLC) is similar to high performance liquid chromatography (HPLC) in principle, but UPLC provides increases in sensitivity and resolution while decreasing run time. To do so, UPLC uses higher pressures compared to HPLC and smaller particle size in columns.

The first step in the separation process is the introduction of the sample containing both analytes into the mobile phase. The mobile phase carries the analytes to the column, where they are retained for a given period of time, and then, usually accompanied by a change in mobile phase composition (though not always necessary), the analytes exit the column separately based on each analyte's polarity. After the analytes are separated, the analytes are transferred to a detector. The Figure 5 below is a diagram of the separation process using UPLC.

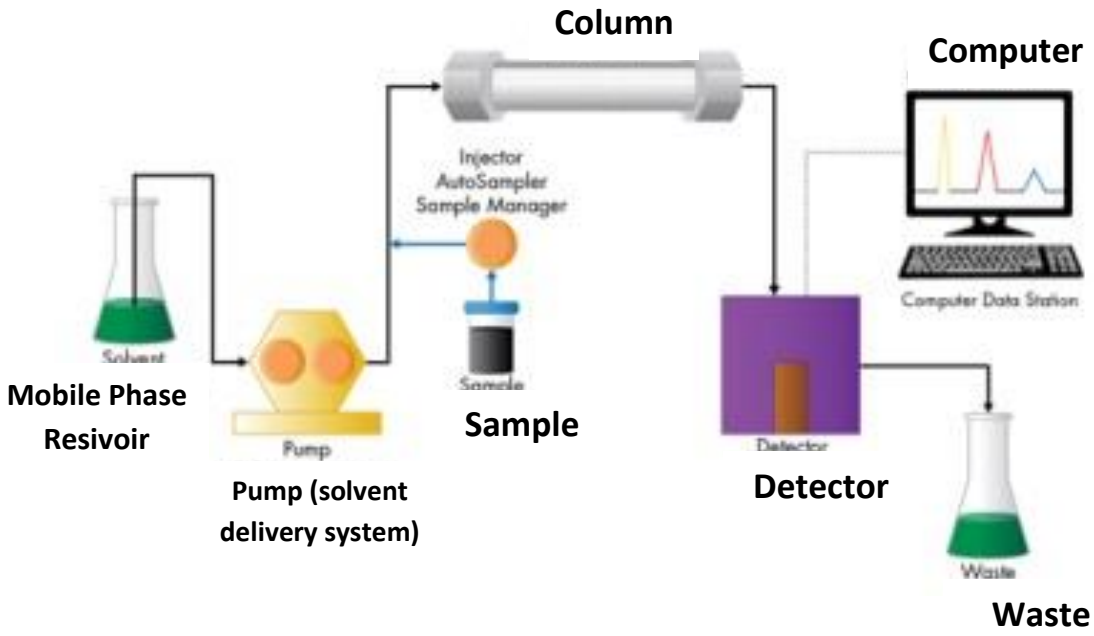

Figure 5: UPLC Schematic. (obtained from Waters Beginner Guide to UPLC; http://www.waters.com/waters/en_US/Chromatographic-Bands%2C-Peaks-and-Band-Spreading/nav.htm?cid=134803614)

For the purposes of this project, the detector is a triple quadrupole mass spectrometer. Mass spectrometry allows for the quantification of analytes based on their mass to charge ratio. Each analyte is first ionized via high voltages using a soft ionization technique known as electrospray ionization. The ionized analytes are accelerated into the first quadrupole (Q1). The first quadrupole serves as the first mass filter based on the analyte's given mass to charge ratio (*m/z*). The ionized analytes filtered through Q1 are denoted the parent ions. The second quadrupole (q2) is the collision chamber; here the selected analytes that pass through Q1 collide with an inert gas, in this case argon gas, inducing fragmentation of the parent ions. The fragmented ions, or daughter ions, are accelerated into the third quadrupole (Q3) where an additional mass filtering occurs.

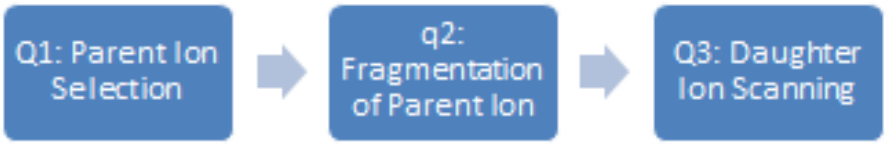

Figure 6: Triple Quadrupole Mass Spectrometry Overview.

For this project, multiple reaction monitoring (MRM) was employed in order to provide lower detection limits, thus increasing the sensitivity of the assay by increasing the specificity of the mass filtering process in Q3. MRM provides lower detection limits and increased sensitivity through the specified filtering of all ions in Q3 except a selected daughter ion, providing a single, specific mass transition that is arguably unique for an analyte. Only this specific transition is

detected, which leads to increased sensitivity and a decrease in noise. A schematic of MRM/MS is shown below.

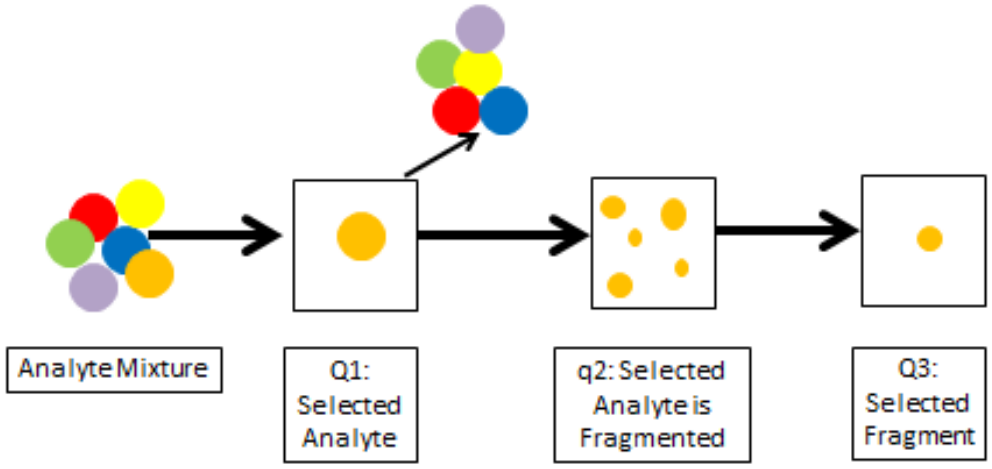

Figure 7: Schematic of Multiple Reaction Monitoring.

Hydrophilic Interaction Liquid Chromatography (HILIC)

Hydrophilic interaction liquid chromatrography (HILIC) is a relatively new chromatography method that allows for the separation of polar analytes. Due to the polarity of both analytes, specifically Tobramycin, this study employed the usage of HILIC. In HILIC the stationary phase is polar, allowing for retention of polar analytes. Typical stationary phase particles include silica, amino, or cyano (Buszewski et al. 2011). Because the retention of polar analytes increases with decreasing polarity of the mobile phase, the typical separation method is a mobile phase gradient ranging from a low polarity organic solvent to a highly polar aqueous solvent. Analytes are separated from the stationary phase in order of increasing polarity.

Methods and Materials

UPLC-MS/MS Method

Using a Waters Acquity ultra performance liquid chromatograph interfaced to a Quattro Micro triple quadrupole mass spectrometer (UPLC-MS), an assay was developed in order to quantify Tobramycin and Vancomycin. The antibiotics were analyzed in the positive ion electrospray mode (ESI+). In addition multiple reaction monitoring (MRM) detection was employed in order to decrease sample noise. For the purpose of analysis, the parent ion for tobramycin was found to be 468.0 *m/z*, signifying the singly protonated, $[M+H]^{+}$, parent ion, and the parent ion for vancomycin was determined to be 725.8 *m/z*, or the doubly protonated $[M+2H]^{+2}$ parent ion. The MRM transition for tobramycin was determined to be 468.4 *m/z* to 163.0 *m/z*, and the MRM transition for vancomycin was determined to be 725.8 *m/z* to 144.3 *m/z*. Figure 8 shows a sample mass spectrum of a 50 ppm vancomycin and tobramycin solution in MQ. Figures 9 and 10 show the fragmentation for vancomycin and tobramycin displaying both the parent and daughter ions for each antibiotic.

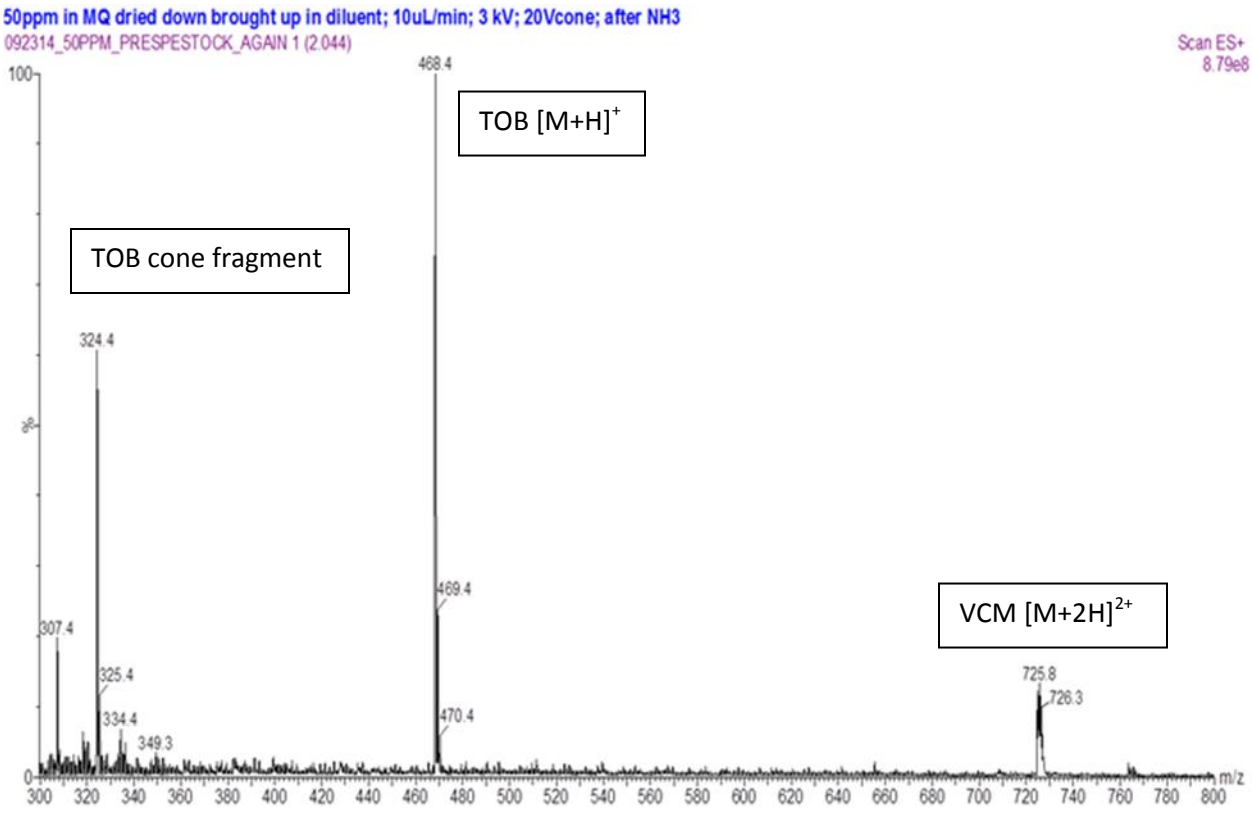

Figure 8: Mass spectrum of Tobramycin (468.4 m/z) and Vancomycin (725.8 m/z) obtained via direct injection. Note 324.4 m/z is a fragment of tobramycin induced by the cone voltage.

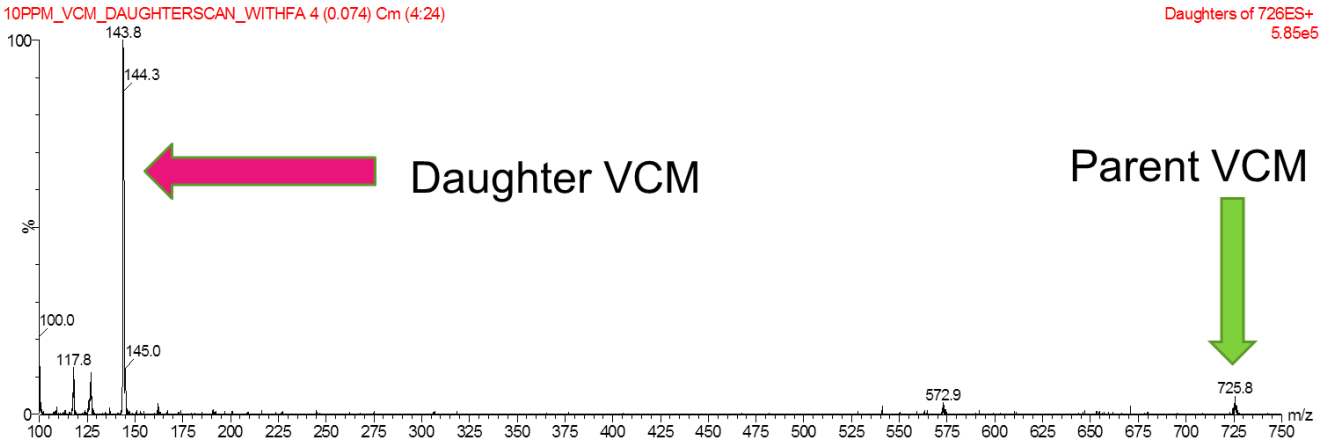

FIGURE 9: Daughter Ions of Vancomycin. The Vancomycin transition was determined to be 725.8 m/z to 144.3 m/z.

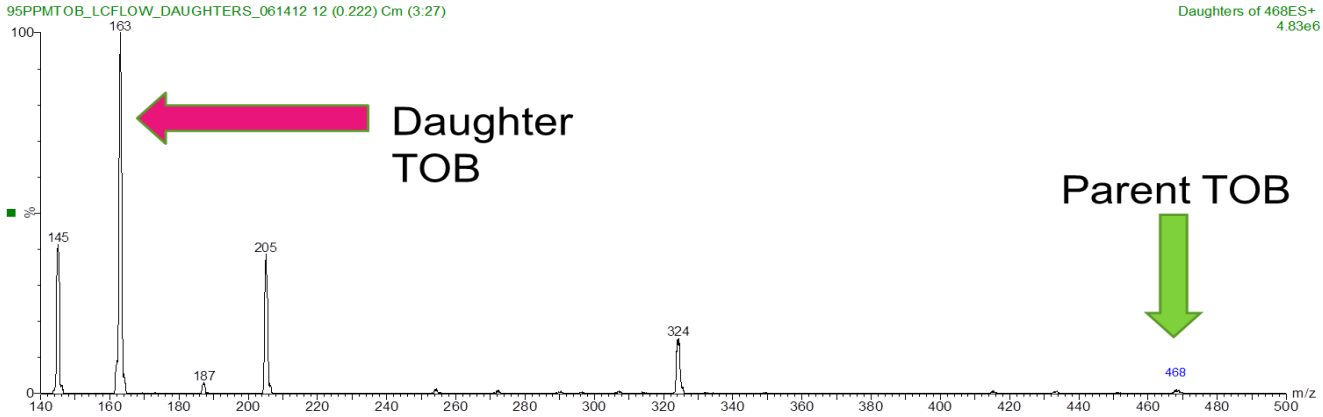

FIGURE 10: Daughter Ions of Tobramycin.The Vancomycin transition was determined to be 468.4 *m/z* to 163.0 *m/z*.

Due to the highly polar nature of both vancomycin and more specifically tobramycin, traditional reverse-phase chromatography using a C18 column was unsuccessful; with reverse-phase chromatography, we were unsuccessful to retain tobramycin. We then turned to hydrophilic interaction liquid chromatography (HILIC) in order to provide better retention for tobramycin. Unlike in reverse-phase chromatography, in HILIC the aqueous solvent is considered

the strong solvent. A Waters BEH amide column was used. The BEH amide column ligand type is a trifunctional amide, which provides retention for highly polar analytes such as tobramycin.

In order to accurately determine peak areas, baseline separation of vancomycin and tobramycin had to be obtained. To do so, the mobile phase composition and gradient along with the sample diluent were optimized. Quantitation is based on external calibration curves using integrated peak areas. For the purposes of method development, pure antibiotic standards are dissolved in 75 Acetonitrile:25 MiliQ Water:0.1 Formic Acid. Mobile phase A is 0.1% Formic Acid in MiliQ Water. Mobile phase B is 0.1% Formic Acid in Acetonitrile. Table 2 shows the optimized gradient, and Figure 11 is a sample chromatogram with attached gradient profile displaying the percent of mobile phase B as a function of time. It is important to note that from Figure 11, as the percent composition of mobile phase B decreases, both analytes are eluted from the BEH column. All solvents are Fisher Optima brand, the highest purity and a requirement of high quality LC-MS work. The method is shown to be linear from 1 – 5 ug/mL. The limit of detection (LOD) for both vancomycin and tobramycin is 500 ng/mL.

Table 2: Optimized gradient for LC-MS

Flow Rate (mL/min)	Time (min)	% Mobile Phase B
0.4	0.0	60
0.4	0.4	60
0.4	1.0	20
0.4	2.0	20
0.4	2.01	60
0.4	4.0	60

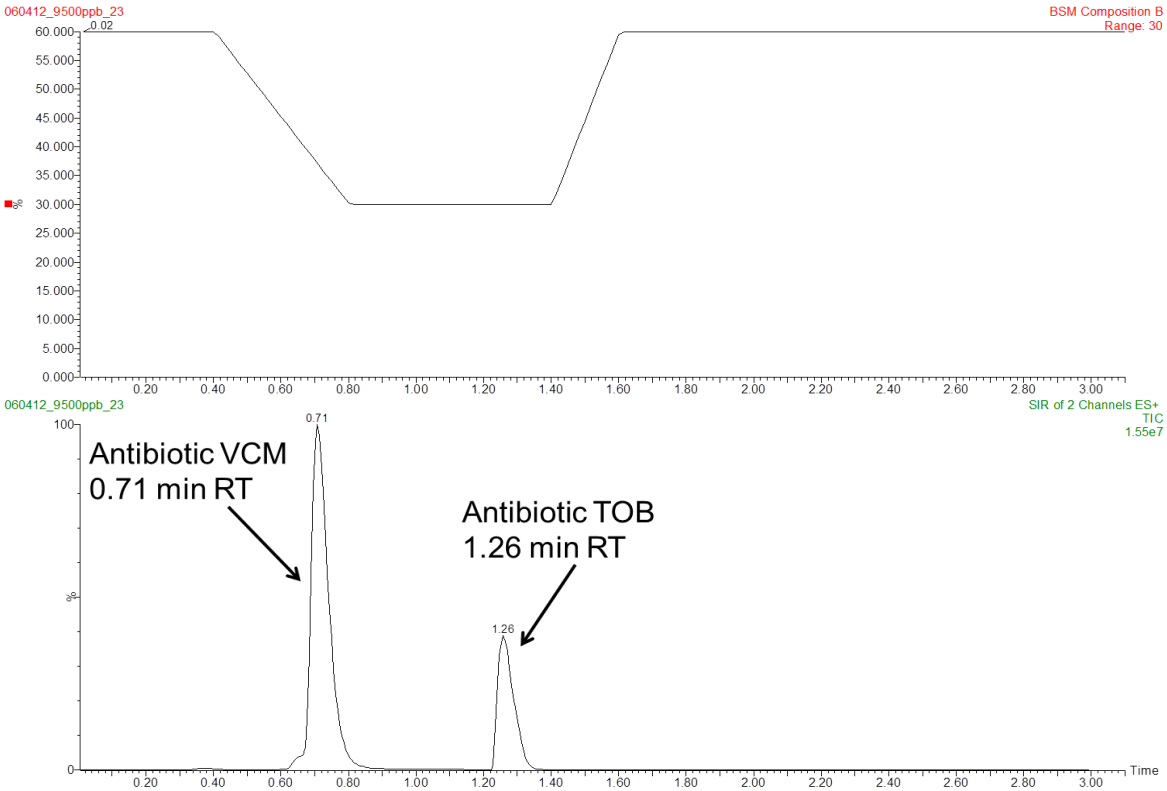

FIGURE 11: Sample Chromatogram (9.5 ppm each analyte) and Optimized Mobile Phase Gradient.

Figures 12 and 13 are sample standard calibration curves for tobramycin and vancomycin respectively.

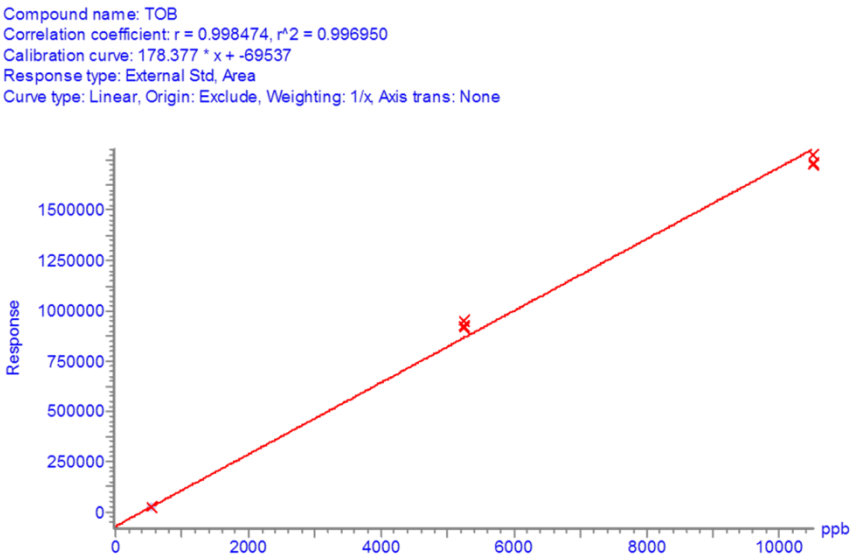

Figure 12: Calibration Curve for Tobramycin using 500 ppb, 5 ppm, and 10 ppm standards.

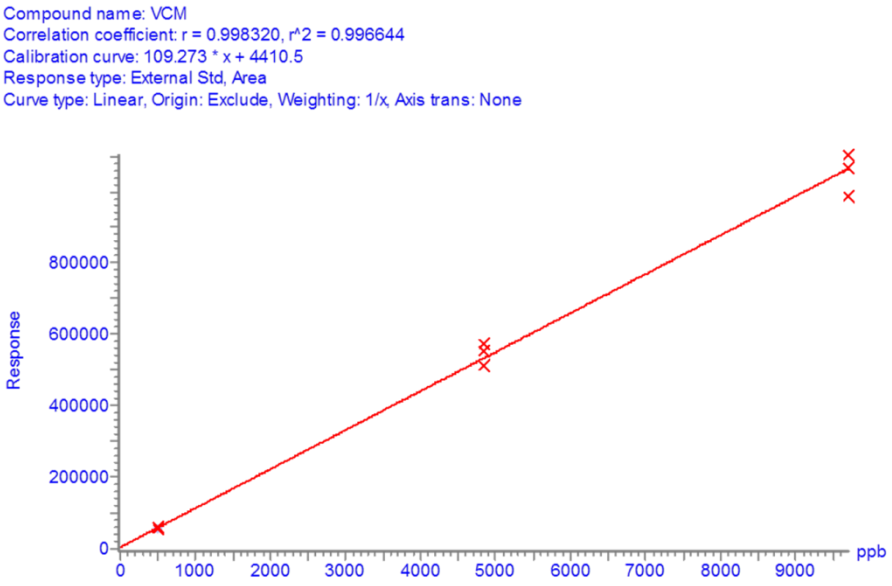

Figure 13: Calibration Curve for Vancomycin using 500 ppb, 5 ppm, and 10 ppm standards.

Antibiotics Study

Six different permutations of electrospun nanofiber devices were received from eSpin, a local Chattanooga company, in order to analyze the release rate of antibiotic as a function of time. The compositions of the six devices are displayed in Table 3 below.

Table 3: Nanofiber Permutations for Antibiotic Study

Sample ID	Composition
13-B1-122-02	98% PLGA + 2% TOB
13-B1-122-03	98% PLGA + 2% VCM
13-B1-122-06	77.5% PLGA + 20% Collagen + 0.5% HA + 2% TOB
13-B1-122-07	77.5% PLGA + 20% Collagen + 0.5% HA + 2% VCM
13-B1-122-08	95.5% PLGA + 0.5% HA + 2% TOB + 2% VCM
13-B1-808-1A	76.59% PLGA + 19.27% Collagen + 0.47% HA + 1.84% TOB + 1.84% VCM

Upon receipt of the nanofiber permutations, approximately a 50 mg square was cut from each permutation, and the exact mass of each was recorded, as displayed in Table 4.

Table 4: Mass of Nanofibers for Antibiotic Study

Sample	Mass (mg)
13-B1-122-02	51.34
13-B1-122-03	56.91
13-B1-122-06	42.94
13-B1-122-07	51.63
13-B1-122-08	60.84
13-B1-808-1A	54.98

Cut and massed nanofiber squares were submerged in 10.0 mL of MiliQ Water (MQ) and incubated at 37°C in order to mimic physiological conditions. In the future, after the solid phase extraction method (SPE) is optimized, this process should be repeated with a phosphate buffered saline (PBS) in replacement of MQ Water. The SPE process is crucial in order to remove primarily phosphate which is present in PBS seeing as phosphate is not volatile and thus cannot enter the mass spectrometer Ideally, samples should be assayed at specific time intervals ranging from 0 hours to 12 weeks, but after experiencing numerous battles with computer failure and instrument failure, the antibiotic study came to a halt, and data was only collected until the 380 hour mark. At the given time interval, the MQ water, containing the eluted antibiotic(s), is decanted into a separately labeled micro-centrifuge tube, and a fresh 10.0 mL of MQ water is added to the tube containing the nanofiber sample. Then, the nanofiber sample is placed back in the incubator until the next time interval. Samples were then analyzed using the

UPLC-MS/MS method as described previously; elution profiles for each nanofiber permutation were then generated.

Mass Loss, pH Study, and Morphological Changes

The experimental methods for the mass loss study were almost identical to those of the antibiotics release rate study. For the mass loss study, three permutations of the nanofiber device were received and tested; the compositions of the three nanofiber devices are listed in Table 5 below.

Table 5: Mass Loss Nanofibers

Sample Name	Composition	Notes
13B1290S1	99.5% PLGA(50/50) + 0.5% HA	0.8 mm thick
13B1296S1	80% PLGA(50/50) + 19.5% Collagen + 0.5% HA	0.3 mm thick
14B2076	80% PLGA (50/50) + 20%Collagen	1 mm thick Alternating layers

After the three nanofiber devices were received, 12 squares were cut from each permutation, to total 36 squares of nanofiber in all. Each square was approximately 50 mg. The original mass of each square was recorded, and each nanofiber square was placed in 10.0 mL of PBS; samples were then incubated at 37°C for a designated period of time. After one week, the PBS for each sample was replaced with a fresh aliquot of 10.0 mL of PBS, and the pH of the decanted PBS was

measured. One sample from each nanofiber permutation was removed from the PBS and allowed to dry. This was denoted the “week one” mass loss sample. Once the nanofiber sample was completely dry, a final mass was recorded and compared to the original starting mass in order to obtain a percent mass loss overall after one week. This process was repeated for a total of 12 weeks; a mass loss profile was generated for each nanofiber permutation over the course of 12 weeks, and simultaneously the pH of the PBS was monitored each week to ensure the nanofiber sample was subjected to physiological pH conditions.

After the mass loss data was collected, morphological changes to the nanofiber sample was studied via scanning electron microscopy (SEM); ultimately, the overall goal of monitoring morphological changes to the nanofiber device is an effort to better understand the changes to fiber shape and porosity, including inter-strand porosity and intra-strand porosity, along with fiber integrity as a function of time in physiological conditions. To do so, samples are gold coated and then imaged in the SEM. These images were then compared to images of the original nanofiber without exposure to physiological conditions.

Results and Discussion

Antibiotics Study

Figures 14 and 15 below show the established elution profiles for both vancomycin and tobramycin as a function of time represented as antibiotic peak area counts as a function of time.

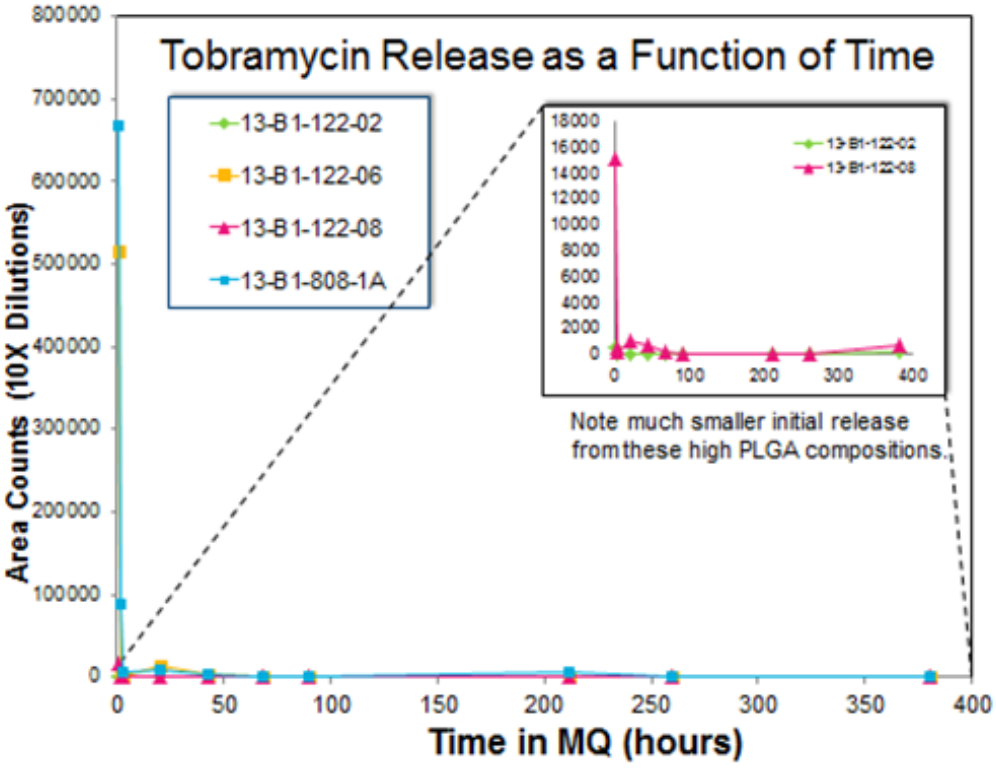

Figure 14: Tobramycin release rate as a function of time in MiliQ Water.

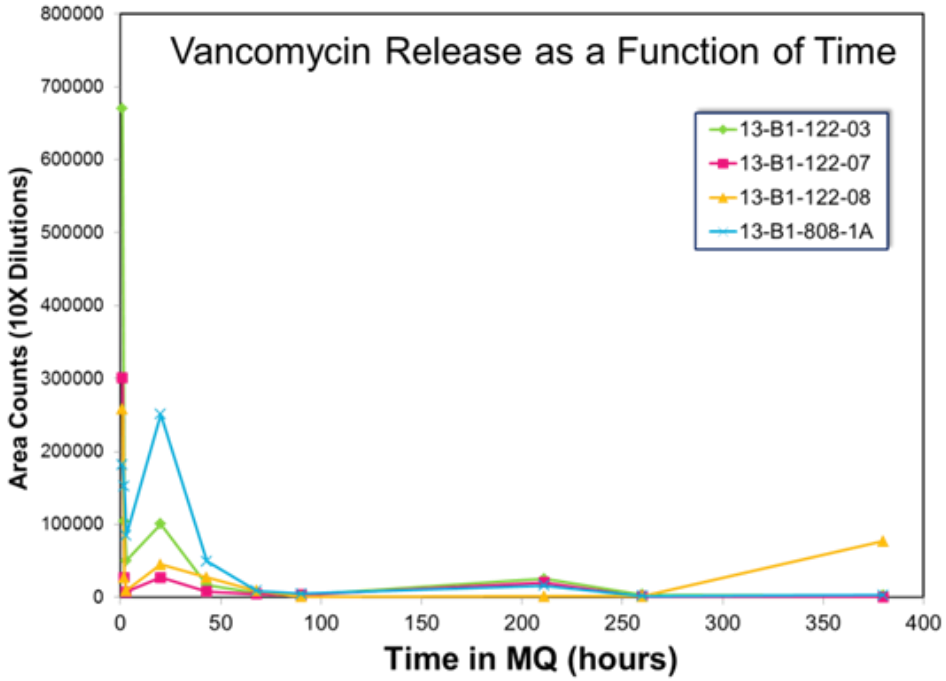

Figure 15: Vancomycin release rate as a function of time in MiliQ water.

Sample 13-B1-122-02, consisting of only PLGA and tobramycin, shows little to no release of tobramycin throughout the first 380 hours. Sample 13-B1-122-06, also containing only tobramycin, shows a large initial release of antibiotics followed by a small release around the 20 hour time point. The notable difference between sample 13-B1-122-02 and 13-B2-122-06 is the presence of both collagen and hydroxyapatite in 13-B2-122-06; the presence of collagen and hydroxyapatite is seemingly linked to a large initial burst of tobramycin. The two samples without tobramycin, containing only vancomycin, were 13-B1-122-03 and 13-B1-122-07; 13-B1-122-03 does not contain hydroxyapatite or collagen, and displays a larger overall release of vancomycin than 13-B1-122-07 which does contain hydroxyapatite and collagen. 13-B1-122-08

consists of PLGA, HA, and both tobramycin and vancomycin; 13-B1-122-08 displays little to no release for tobramycin, and small releases of vancomycin, with a notable increase in release between the 260-380 hour time points. Lastly sample 13-B1-808-1A, composed of PLGA, collagen, HA, tobramycin, and vancomycin, gave a large initial release of tobramycin and vancomycin; after the initial burst of tobramycin, little to no tobramycin was released. For sample 13-B1-808-1A, the initial release of vancomycin is accompanied by a secondary, larger release of antibiotic, and then followed by only small releases of antibiotic. Table 6 below summarizes the antibiotic elution rates for both antibiotics in all six permutations of nanofiber devices received.

Summary- Release over 380 hours

Sample	Release of TOB	Release of VCM
13-B1-122-02	Little to none	Not present in fiber
13-B1-122-03	Not present in fiber	1 hour: largest burst 20 hour: 2nd largest burst 20-380 hours: little
13-B1-122-06	Large initial burst, followed by little	Not present in fiber
13-B1-122-07	Not present in fiber	1 hour:2nd largest release 20 hour: smallest release 20-380 hours: little release
13-B1-122-08	Little to none	1 hour: smallest release 20 hour: 3rd highest release 380 hour: small burst
13-B1-808-1A	Large initial burst, followed by little	1 hour: 3rd largest burst 20 hour: largest burst 20-380 hours: little

Table 6: Antibiotic Elution Summary

Results obtained from the antibiotic study are similar to previously documented elution rates from other nanofiber device studies. One study involving the incorporation of Mefoxin®, a hydrophilic antibiotic, into a nanofiber scaffold, reports large initial bursts of antibiotic in which the majority of the antibiotic was released within the first hour (Kim et al. 2004). Similarly another study reported almost 90% of the incorporated gentamicin, an aminoglycoside antibiotic, in a nanofiber scaffold was eluted within the first hour (Sirc et al. 2012). Suggested rationale for this rapid release is due to the adsorption of the hydrophilic antibiotics to the surface of the nanofiber mesh (Kim et al. 2004). Documented observations by eSpin stating the difficultly incorporating the antibiotics into the nanofiber mesh accompanied by the rapid release of antibiotic suggest that antibiotics in this study, particularly tobramycin, are simply adsorbed to the nanofiber mesh surface instead of being incorporated into the mesh.

Mass Loss Study

The results of the mass loss study are shown below in Figure 16. 13B1290S1 is the slowest of the three fibers to degrade, suggesting that the presence of collagen speeds up the rate of degradation as displayed in both 14B2076 and 13B1296S1. 14B2076 and 13B1296S1 display similar mass loss profiles, suggesting that the presence of hydroxyapatite has little impact on degradation as to be expected.

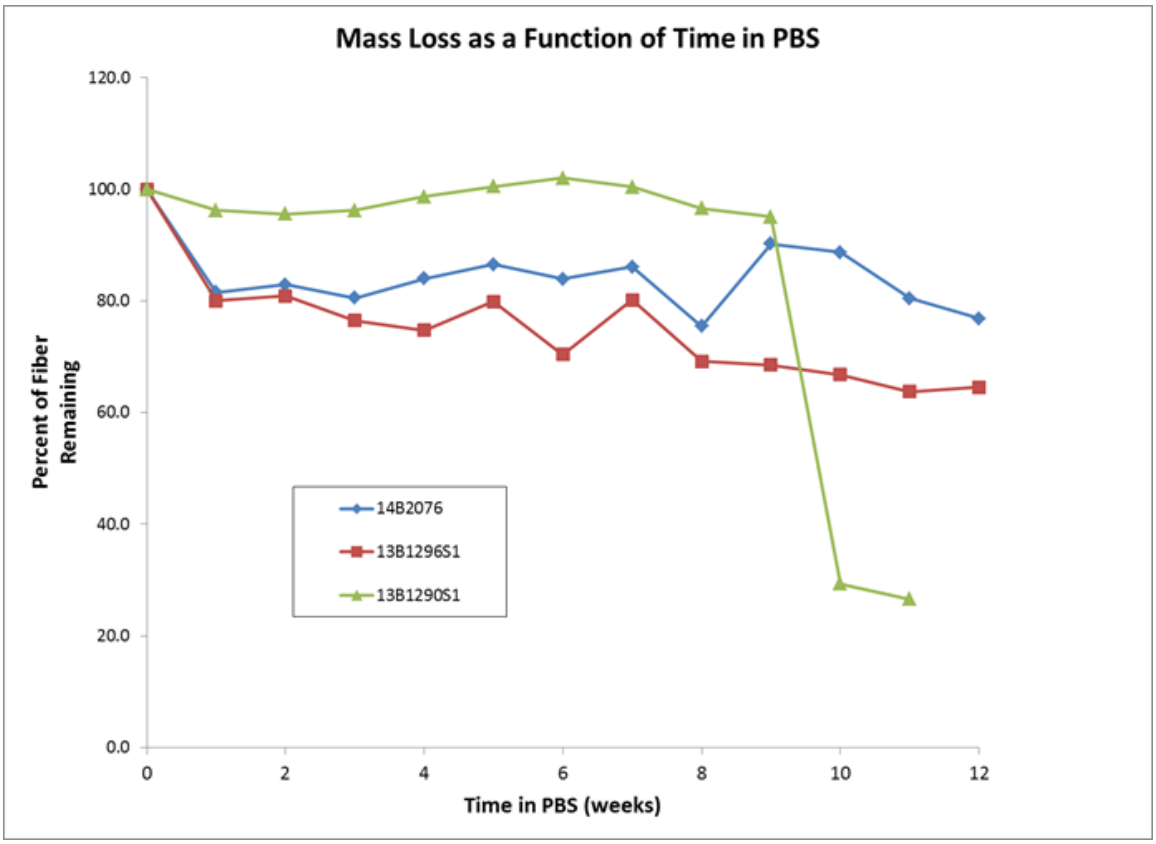

Figure 16: Mass loss of 14B2076, 13B1296S1, and 13B1290S1 as a function of time in PBS.

As seen in Figure 17 above, there appears to be an increase in mass in multiple samples, primarily in later weeks. This is believed to be due to inadequate drying time of the nanofiber sample. Ultimately the drying technique of the samples needs to be optimized and the overall mass loss study repeated with this optimized technique.

pH Study

As mentioned previously, pH changes were also monitored in addition to mass loss. Shown below is a graph displaying the change in pH as a function of time in PBS (Figure 16). The pH remains fairly constant in the 13B1290S1 samples, until week 10; the pH drop is most likely due to increased degradation, seeing as this corresponds to the dramatic mass loss represented in Figure 16 above. It is important to note that the degradation of PLGA yields both lactic and glycolic acids which could cause a decrease in pH with the overall increase of acidity.

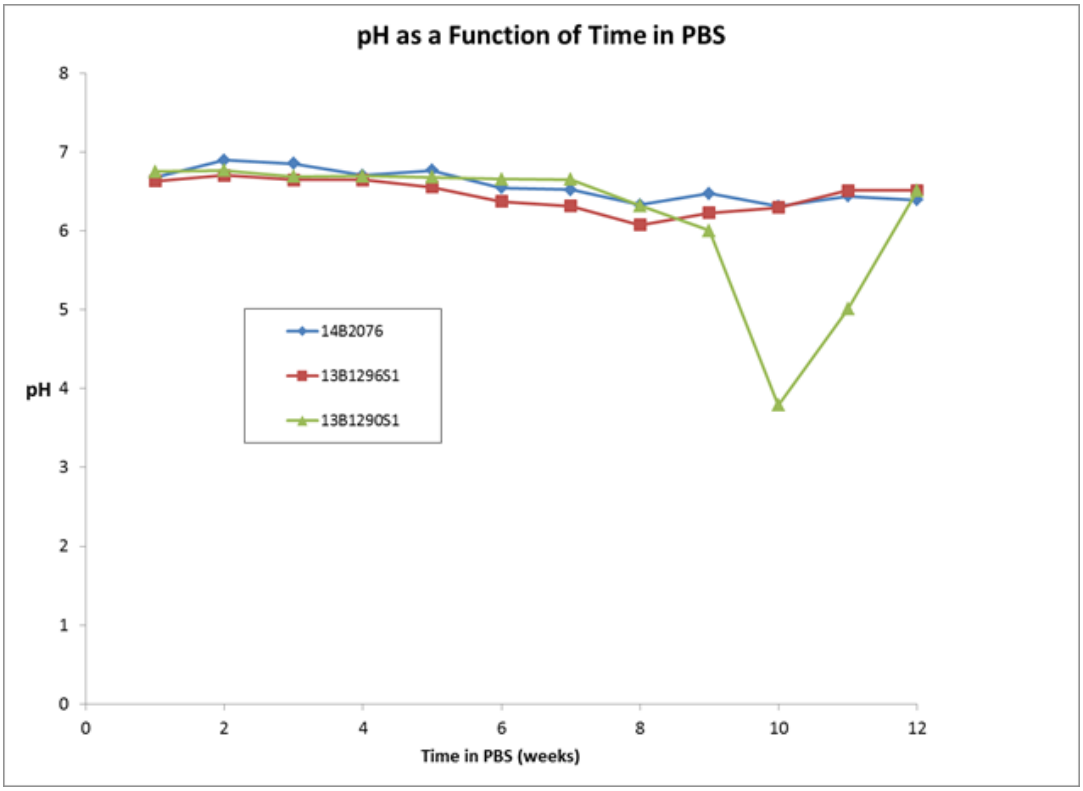

Figure 17: pH of PBS as a function of nanofiber incubation time.

Morphological Changes

Using a scanning electron microscope, morphological changes to the nanofiber mesh for each nanofiber mesh permutation was documented as a function of incubation time. Figure 18 below is the week 0 SEM image for sample 14B2076; it is important to note that this sample of 14B2076 has not been exposed to PBS. The unperturbed 14B2076 sample is characterized by spherical accretions, most likely consisting of collagen, and varying pore size, and varying fiber diameter. As the 14B2076 sample is exposed to physiological conditions, the fibrous nature of the nanofiber mesh is lost as the strands fuse together to produce a matte, and there is a notable increase in inter-strand porosity. The effects of exposure to physiological conditions on

14B2076 are shown in the week 2, week 5, and week 10 samples in Figures 19, 20, and 21 below.

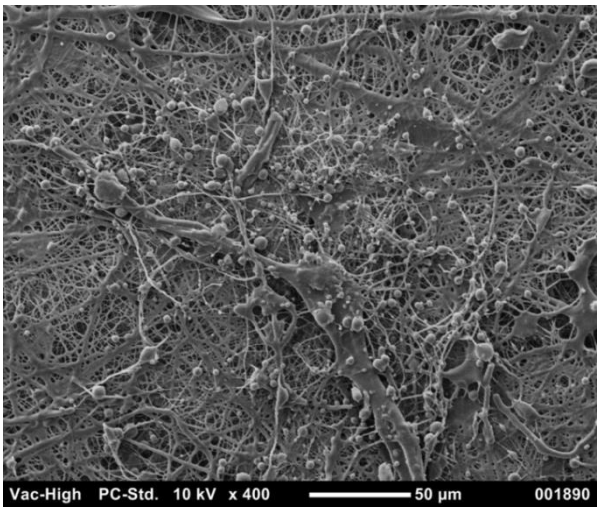

Figure 18: 14B2076 Week 0 SEM Image .

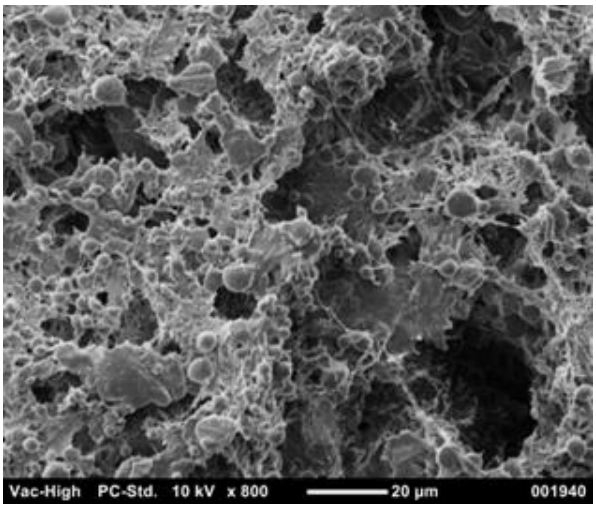

Figure 19: 14B2076 Week 2 SEM Image.

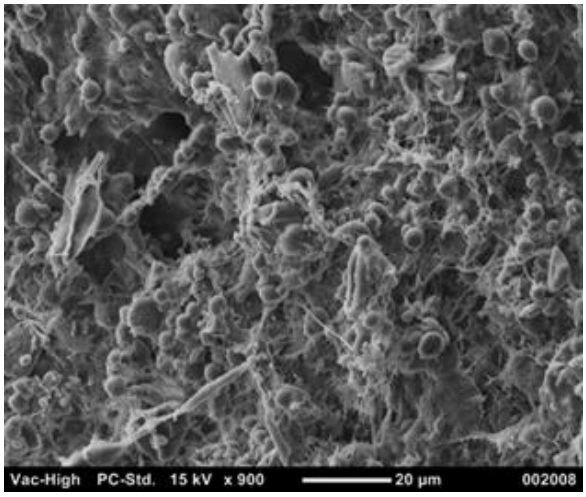

Figure 20: 14B2076 Week 5 SEM Image.

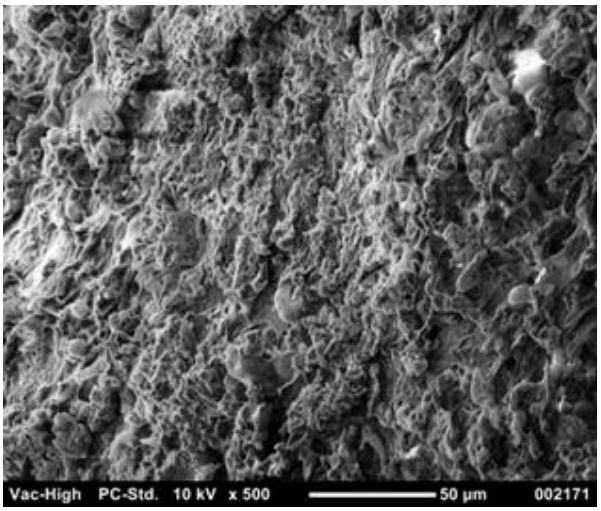

Figure 21: 14B2076 Week 10 SEM Image.

The 13B1296S1 sample at week 0 contains large, flat, ribbon-like strands, most likely composed of collagen, and is characterized by small inter-strand pores. Figure 22 shows the week 0 sample for 13B1296S1. As 13B1296S1 is exposed to physiological conditions, intra-strand pore size increases dramatically and similarly to 14B2076 there is an overall loss of fibrous nature; however in the case of 13B1296S1, the loss of fibrous nature is due to fiber splitting, creating a budding effect.

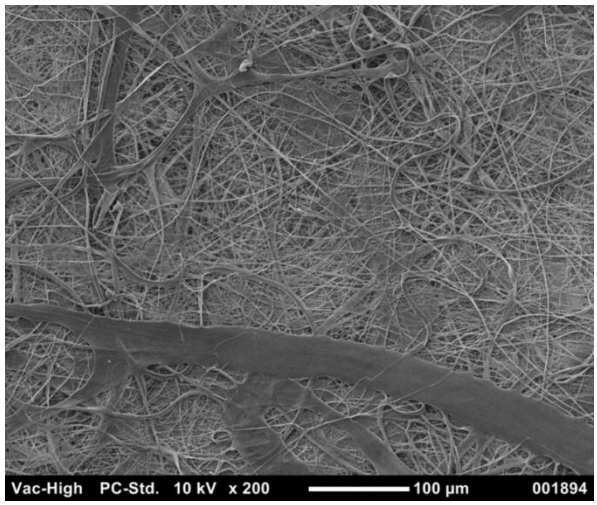

Figure 22: 13B1296S1 Week 0 SEM Image

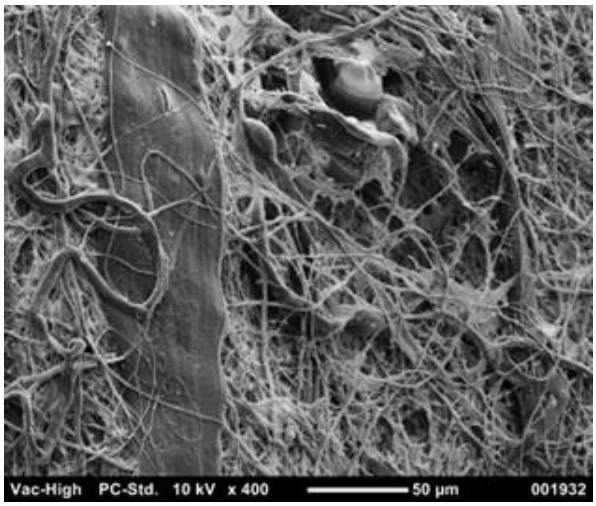

Figure 23: 13B1296S1 Week 2 SEM Image

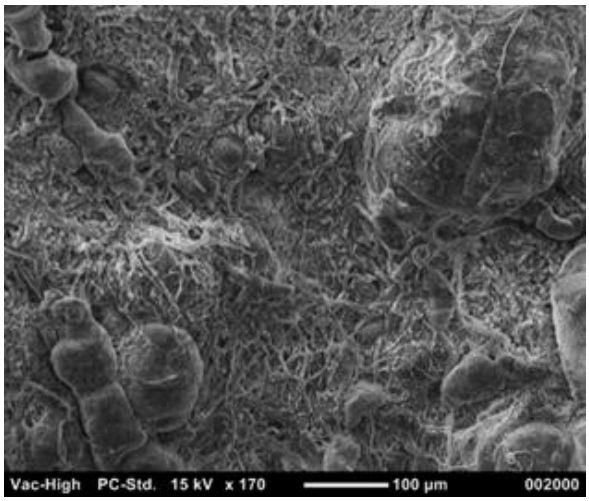

Figure 24: 13B1296S1 Week 5 SEM Image

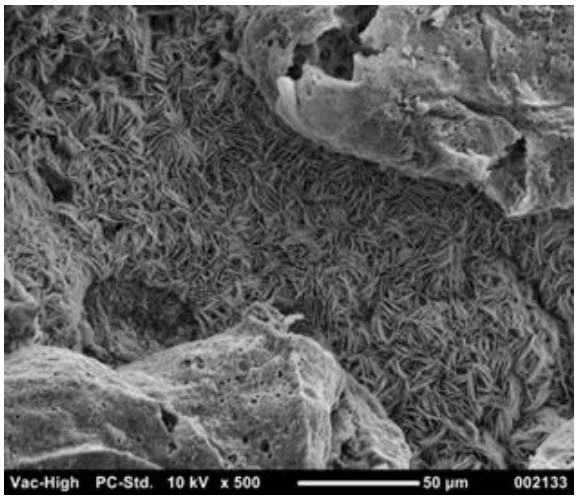

Figure 25: 13B1296S1 Week 10 SEM Image

The 13B1290S1 sample at week 0 is extremely uniform with average fiber diameter of 0.5-1.0 microns. As 13B1290S1 is exposed to physiological conditions, intra-strand and inter-strand pore sizes increase, and again there is an overall loss of fibrous nature due to fiber splitting, similar to the splitting shown in 13B1296S1. By week 10, sample 13B1290S1 is difficult to retrieve and image due to dramatic mass loss resulting in extreme fragmentation; at this point, there is no remaining fibrous nature in the sample as it appears matte-like.

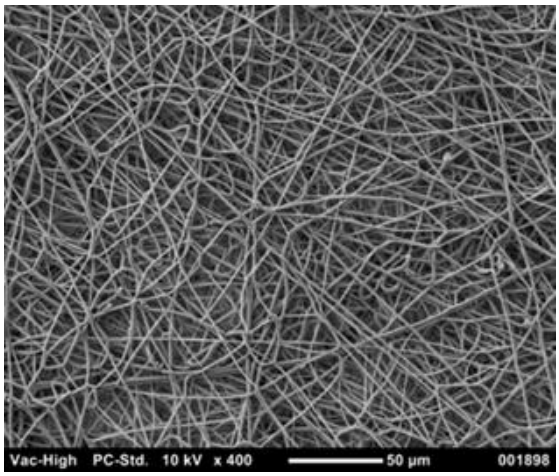

Figure 26: 13B1290S1 Week 0 SEM Image

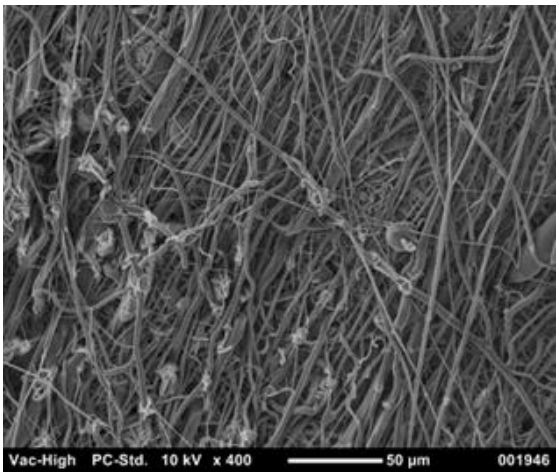

Figure 27: 13B1290S1 Week 2 SEM Image

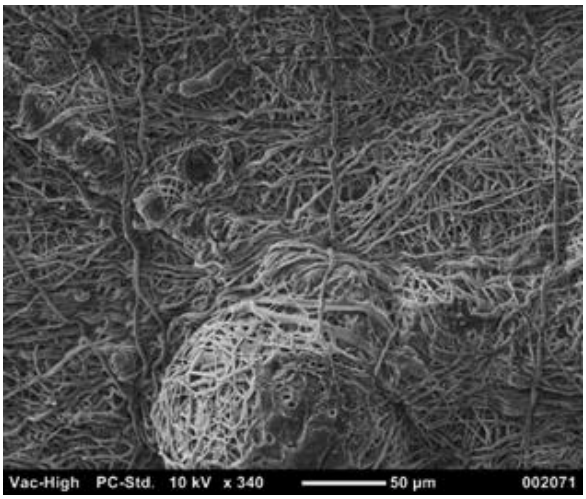

Figure 28: 13B1290S1 Week 5 SEM Image

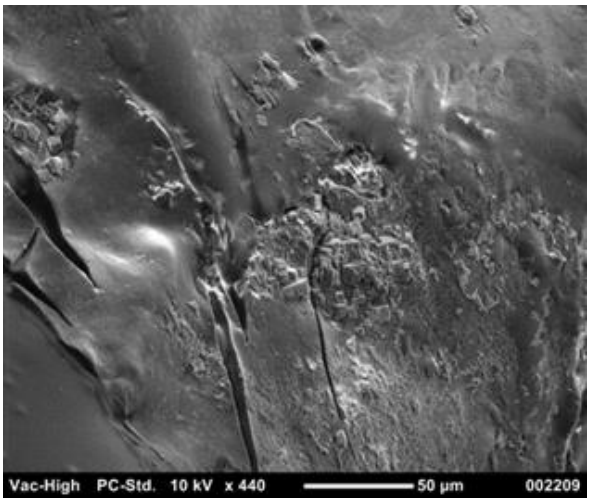

Figure 29: 13B1290S1 Week 10 SEM Image

Comments and Future Work

In the future, the primary goal is to revisit the antibiotic release rate study. As soon as the SPE method is optimized, the antibiotic study needs to be revisited. With an optimized SPE method it will be possible to conduct the entire antibiotic elution study using PBS instead of MQ, ultimately providing more accurate data since the PBS more closely mimics physiological conditions.

Currently, a pilot study on rabbits with the three nanofiber permutations listed in Table 5 is underway. Upon the results of the rabbit study, the mass loss study will be revisited as well. The most successful nanofiber permutation determined from the rabbit study will be extensively analyzed. The mass loss of this nanofiber permutation as a function of time will be documented. The samples in the future mass loss study will be done in triplicate and will be subjected to the optimized drying procedure.

Lastly, the rapid elution of antibiotics needs to be addressed via nanofiber device modifications. The ideal elution profile includes a large initial burst of antibiotics shortly after surgery in order to prevent a bacterial infection from colonizing followed by a sustained release of antibiotics to combat the remaining bacteria not eliminated with the initial antibiotic release (Kim et al. 2004). To obtain a more sustained release of antibiotics, nanofiber diameter could be increased, or the nanofiber mesh thickness could be increased (Kim et al. 2004). By increasing the nanofiber mat thickness, the porosity of the overall mesh decreases, allowing for greater retention of antibiotics (Sirc et al. 2012). Additionally, the usage of buffering nanofiber cover meshes could be employed, essentially creating a layered nanofiber mesh. A multi-layered nanofiber device with thicker covering layers could further increase antibiotic retention, allowing for a more sustained release (Sirc et al. 2012).

References

1. Barth, R. E.; Vogely, H. C.; Hoepelman, A. I. M.; Peters, E. J. G. 'To bead or not to bead?' Treatment of osteomyelitis and prosthetic joint-associated infections with gentamicin bead chains. *International Journal of Antimicrobial Agents*, **2011**, 38, 371-375.
2. ChemAxon, www.chemicalize.org , (accessed on March 19, 2015).
3. Dodd, M. C.; Buffle, M. O.; Von, G. U. Oxidation of antibacterial molecules by aqueous ozone: moiety-specific reaction kinetics and application to ozone-based wastewater treatment. *Environmental Science & Technology,* **2006**, 40(6), 1969-77.
4. Friess, Wolfgang. Collagen – biomaterial for drug delivery. *European Journal of Pharmaceutics and Biopharmaceutics.* **1998**, 45, 113–136.
5. Gao, Y.; Cao, W. L.; Wang, X. Y.; Gong, Y. D.; Tian, J. M.; Zhao, N. M.; Zhang, X. F. Characterization and osteoblast-like cell compatibility of porous scaffolds: bovine hydroxyapatite and novel hydroxyapatite artificial bone. *Journal of Materials Science*: *Materials in Medicine*, **2006**, 17(9), 815-823.
6. Jaffe, G.; Yang, C.Hao; Guo, H.; Denny, J. P.; Lima, C.; Ashton, P. Safety and Pharmacokinetics of an Intraocular Fluocinolone Acetonide Sustained Delivery Device. *IOVS*, **2000**, 41(11), 3569-3575.
7. Kim, K.; Luu, Y. K.; Chang, C.; Fang, D.; Hsiao, B. S.; Chu, B.; Hadjiargyrou, M. Incorporation and controlled release of a hydrophilic antibiotic using poly(lactide-co-glycolide)-based electrospun nanofibrous scaffolds. *Journal of Controlled Release*, **2004**, 98, 47–56.

8. Makadia, H. K.; Siegel, S.J. Poly Lactic-co-Glycolic Acid (PLGA) as Biodegradable Controlled Drug Delivery Carrier. *Polymers*, **2011**, 3(3), 1377-1397.

9. Okuda, T.; Tominaga, K.; Kidoaki, S. Time-programmed dual release formulation by multilayered drug-loaded nanofiber meshes. *Journal of Controlled Release*, **2010**, 143, 258–264.

10. Pignatello, R.; Mangiafico, A.; Basile, L.; Ruozi, B.; Furneri, P. M. Amphiphilic ion pairs of tobramycin with lipoamino acids. *European Journal of Medicinal Chemistry,* **2011**, 46(5), 1665-1671.

11. Samuel, S.; Ismavel, R.; Booplan, P.; Matthai, T. Practical considerations in the making and use of high-dose antibiotic-loaded bone cement. *Acta. Orthop. Belg*., **2010,** 76, 543-545.

12. Sirc, J. et al. Controlled gentamicin release from multi-layered electrospun nanofibrous structures of various thickness. *International Journal of Medicine*, **2012**, 7, 5315-5325.

13. Waters Beginner's Guide to UPLC; http://www.waters.com/waters/en_US/Chromatographic-Bands%2C-Peaks-and-Band-Spreading/nav.htm?cid=134803614 (accessed March 16, 2015).

14. Yang, C. Y. et al. Intramedullary implant of plasma-sprayed hydroxyapatite coating: An interface study. *Journal of Biomedical Materials Research*, **1997,** 36(1), 39-48.

15. Zhang, T. et al. Determination of vancomycin in serum by liquid chromatography–high resolution full scan mass spectrometry. *J. Chromatogr*., **2007**, 857, 352–356.